AC Impedance Analysis of Improved Oxygen Electrodes for Rechargeable Li/Oxygen Batteries

Mojtaba Mirzaeian **(**University of Strathclyde) — Glasgow, Scotland, UK — Mojtaba.mirzaeian@strath.ac.uk

ABSTRACT

The electrochemical performance of the Li/O_2 cells, using polymer based carbons with controlled pore structure as active material in the cathode electrode, was evaluated by galvanostatic charge/discharge cycling and in situ impedance measurements. It was shown that the storage capacity and discharge voltage of Li/O_2 cells strongly depend on the morphology of the carbons used in cathode. Electrochemical impedance spectroscopy results showed that the shape and value of the resistance in the impedance spectrum of Li/O_2 cell is strongly affected by the structure of the cathode. Gradual increase in the cell impedance with cycling, changes the porosity of the electrode and therefore the ability of oxygen and lithium ions to diffuse into the electrode, probably due to the irreversible deposition of some discharge products in the pores of the carbon.

INTRODUCTION

New battery technologies with higher specific energy, lower cost, and longer calendar and cycle lifetimes are required allowing electricity derived from renewable resources to replace fossil hydrocarbons as the primary energy carrier of the transportation sector. While battery-electric vehicles developed in the past, have not been widely successful [1]; and the future development of battery powered vehicles is still slowed down by limitations in battery technology supplying an energy service comparable to hydrocarbon-fueled vehicles; there is intense interest in developing storage technologies with high energy and power densities; and capable of storing and delivering energy with longer service life.

Current rechargeable lithium ion batteries that use lithium cobalt oxide as cathode and graphite as anode play a key role in powering portable electric devices. The specific energy of these energy storage systems is limited mainly by the capacity of the cathode material, which can store only 140 mA h g^{-1} of charge compared to the capacity of 372 mA h g^{-1} for graphite [2]. Although several alternative approaches including new intercalation cathodes [3-6]; alternative anode materials to graphite [7, 8]; polyvalent cations [9]; and oxide electrodes [10] are considered to enhance the storage capacity of lithium ion batteries however these methods either raise serious challenges for reversibility [11, 12] or increase the energy density of the cathode only by a factor of 2 which is not enough to power our modern lifestyles demand [2].

To achieve the goals of using electrical energy in transportation and electricity grid applications a major step change in battery technology is needed, a step that can be taken only by obtaining a fundamental understanding of the physical and chemical processes that occur in these complex systems to enable breakthroughs in charge storage and energy density of current battery technology.

Metal/air batteries have a much higher specific energy than most available primary and rechargeable batteries which is critical for applications that are very sensitive to weight. These power sources couple a metal anode electrochemically to atmospheric oxygen through an air electrode using an aqueous electrolyte and are unique in that molecular oxygen as cathode active material is absorbed from air and is not stored in the battery. Among different metal/air couples such as Zn/air, Al/air, and Mg/air [13-18], the Li/air couple is especially attractive as in principle it should provide one of the highest energy density yet investigated for advanced battery systems [19]. Li/air chemistry combines Li, the less electronegative material with the highest capacity, with oxygen. This system has a theoretical specific energy of 13000 Wh/kg assuming a cell voltage of 3.4 V [20], though only 2.85 V is achieved in practice. Although the aqueous lithium air cells have desirable volumetric and gravimetric energy densities, their broad application is limited by the undesired reaction of lithium with water and corrosion of the anode which is considerable challenge for the practical utilization of these cells [21, 22].

Abraham and Jiang were the first to report a lithium/oxygen cell using a non-aqueous electrolyte [22]. The cell was shown to have an operating voltage of 2.0 to 2.8 V, with a catalytic air electrode recharging over several cycles. The

discharge mechanism was determined to be primarily the deposition of Li_2O_2 in a carbon-based air electrode. This cell design overcomes the corrosion and safety concerns of the past plagued lithium air systems and its operating voltage is higher than that of metal air batteries using aqueous electrolyte, but its cyclability is limited as the end of discharge is reached when insoluble discharge products, Li_2O and Li_2O_2, fill pores of the air cathode electrode [23]. Although several studies have explored the effects of air electrode formulation and electrolyte composition [24], mechanism of charge/discharge catalytic reaction and role of catalyst [2] and optimization of electrode porosity and structure [25] on the performance of organic electrolyte lithium oxygen batteries, but less has been done to understand the impedance characteristics of a lithium oxygen cell in particular less is known about the uniformity of the air electrode with charge/discharge cycling.

In the present study, a resorcinol formaldehyde based carbon with controlled porous structure was synthesized, and its performance as active material in air electrode in a lithium oxygen battery was evaluated. Insitu electrochemical impedance spectroscopy (EIS) has been also applied to study the interfacial changes occurring at the battery electrodes with charge/discharge cycling.

EXPERIMENTAL

Preparation of carbon aerogels and their organic precursors has been described elsewhere [26]. The gel for this study was synthesized at a [Resorcinol] / [formaldehyde] ratio of 0.5 and [Resorcinol] / [Catalyst] ratio of 600. Resorcinol and formaldehyde were mixed with adding appropriate amount of water and sodium carbonate as polymerization catalyst for 45 minutes. The solution was poured into a glass vial, sealed and cured at elevated temperature. After curing for 6 days, the aquagel was solvent exchanged in acetone for 3 days to ensure complete removal of the water from the gel structure. Acetone exchanged RF gel was then filtered and dried at 353K under vacuum for 3 days. The RF aerogel was subsequently pyrolyzed in a tubular furnace under Ar at 1073 K. Activated carbon aerogels were prepared by activation of the resultant carbon under CO_2 at different temperatures and times.

The porosity of RF areogel and carbon aerogels were studied by the analysis of nitrogen adsorption-desorption isotherms measured by an ASAP 2420 adsorption analyzer (Micromeritics) at 77 K. The samples were evacuated at 373 K for 2 hours prior to the adsorption measurements. BET method was used for surface area measurements, BJH adsorptions-desorption was used for mesopore analysis and t-plot method was used for micropore analysis. Total pore volume was calculated from the adsorbed volume of nitrogen at $P/P_0 = 0.99$ (saturation pressure). Pore size distributions were obtained by the BJH method from adsorption branch of the isotherms [27].

Positive cathode electrodes were prepared by mixing milled porous carbon-aerogel, electrolytic manganese dioxide (EMD), Kynar Flex 2801 as binder and propylene carbonate (PC) as wetting agent and then casting in 200µm thick films according to the procedure described elsewhere [23-25]. Electrochemical cells were constructed in an argon-filled glove box using a lithium metal foil as anode, a glass micro-fiber separator soaked with electrolyte (1 M $LiPF_6$ in propylene carbonate) and a disc of 1.3 diameter cathode electrode. The cell parts were compressed together to ensure that the electrode contact is good and then the cell was completely sealed except for the cathode side that exposes the porous cathode to the O_2 atmosphere. The cell then was exposed to O_2 at atmospheric pressure for a minimum of 30 min prior to the electrochemical tests and all measurements were carried out under O_2 atmosphere at 298 K.

Electrochemical performance of the prepared lithium oxygen batteries were examined using a 1470E Solartron cell test system and a 1455 frequency response analyzer. The charge and discharge cycling of the cells were conducted galvanostatically at a 70 mA/g rate in a voltage range of 2.05 to 4.4 V. Electrochemical impedance spectroscopy of the obtained cells was evaluated using an AC impedance analyzer over a frequency range of 10^6 HZ to 10^{-3} Hz for interface investigation of the electrodes in cells after each charge and discharge cycle.

RESULTS AND DISCUSSION

Figures 1 and 2 show the adsorption-desorption isotherms and pore size distribution curves for carbon samples activated at different temperatures. Activated carbons are named as ACRF600-x where x is activation temperature.

Vertical shift in the location of hysteresis loops to higher volumes shows that the amount of gas adsorbed by sample increases with the activation temperature which is indicative of the development of porosity in the carbon structure.

The pore size distribution curves are centred at the same pore diameter range (i.e. around 40 nm) indicating all carbon samples are mainly mesoporous materials and possess similar pore sizes and pore size distributions. Figure 2 and data given in Table 1 show that such an activation treatment results in activated carbons with controlled porosity having high pore volumes with average pore diameters of around 20 nm.

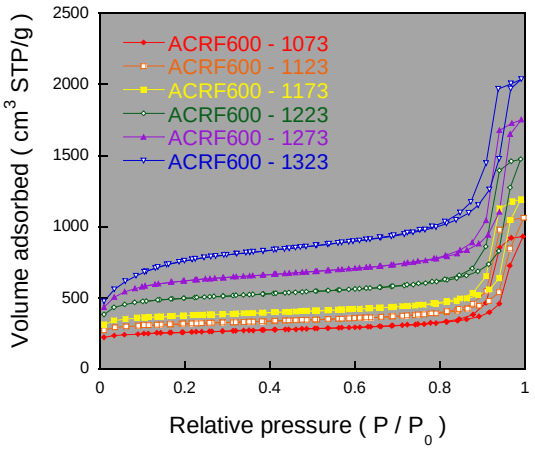

Fig 1. Nitrogen adsorption-desorption isotherms at 77 K for carbons activated at various temperatures.

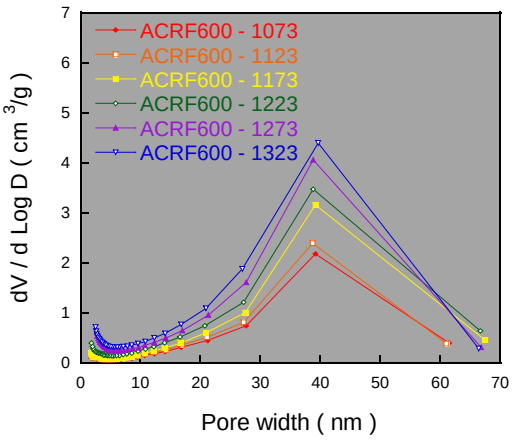

Fig 2. Pore size distribution of carbons activated at various temperatures.

Table 1. Porous parameters of ACRF600 carbon samples activated at different temperatures.

Sample	S_{BET} (m^2/g)	V_{total} (cm^3/g)	V_{micro} (cm^3/g)	V_{meso} (cm^3/g)	$\%V_{micro}$	$\%V_{meso}$	D_{avg} (nm)
ACRF600- 1073K	801	1.441	0.296	1.145	20	80	23.98
ACRF600- 1123K	982	1.641	0.374	1.261	22	78	22.05
ACRF600- 1173K	1555	2.278	0.550	1.728	24	76	20.54
ACRF600- 1223K	1164	1.839	0.437	1.402	23	77	18.37
ACRF600- 1273K	1674	2.375	0.502	1.873	21	79	17.80
ACRF600- 1323K	2471	3.146	0.335	2.811	11	89	17.37

Figure 3 shows discharge behavior of the Li/O_2 cells based on electrodes prepared from ACRF600-x carbons. Variations of the cell voltage against specific capacity of carbon samples at a discharge rate of 70 mA/g show flat discharge profiles at about 2.6-2.8 V. These are associated with the storage behavior of the cells and are in good agreement with the preceding reported data for a similar cell discharged in O_2 at atmospheric pressure involving formation of Li_2O_2 [22, 23]. It can be seen that the storage capacity increases with the development of mesoporosity in carbons. Sample ACRF002- 1323K with higher mesopore volume showed the highest storage capacity and sample ACRF002- 1073K with lower mesopore volume showed the lowest storage capacity between carbon samples. It is believed that larger pore volume provides more space for the formation and storage of Li_2O_2 during the discharge process as the end-of-discharge of the cell is reached when the carbon pores are filled or choked by the deposition of Li_2O_2 [25]. The role of pore size in air electrode is another key factor affecting the cell performance as wider pores might result in higher diffusivity of the electrolyte into the carbon structure, better accessibility of lithium ions to the carbon surface and better diffusion of oxygen onto the carbon-electrolyte interface as charge/discharge reaction sites.

Figure 4 shows the impedance spectra of the lithium/ oxygen cells measured over a span of frequencies ranging from 10^6 Hz to 10^{-3} Hz. The high frequency intercepts at the real Z axis are corresponded to the electrolyte

resistance. The relaxation semicircles are attributed to the formation of discharge products in the air electrode/ electrolyte interface and also include the intrinsic electronic resistance of the carbon electrode and the contact resistance of the carbon particles. The transition region between the relaxation loops and low frequency linear tails might be due to the charge transfer process on the covered electrode. The low frequency linear tails represent diffusion limitation of lithium ions into discharge reaction zone within the electrode (Warburg effect) [28-29].

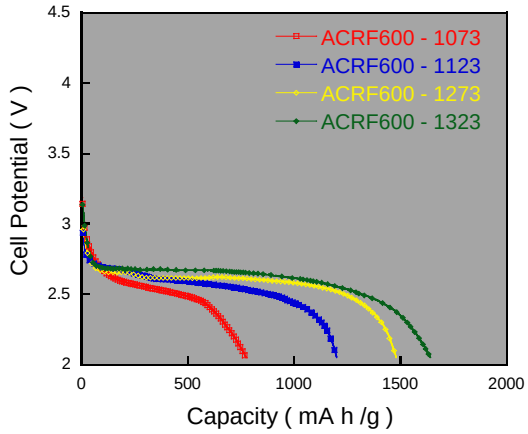

Fig 3. Discharge capacities of ACRF600-x carbons (rate 70 mA/g).

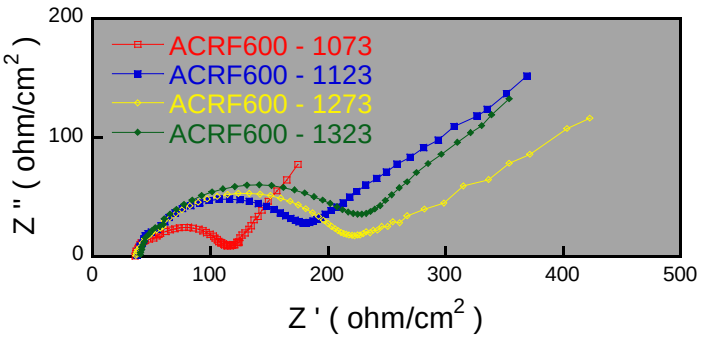

Fig 4. Impedance spectra of carbons after first discharge (rate 70 mA/g).

The shape and value of the resistance in the impedance spectrum is strongly affected by electrolyte and electrode thickness and structure [28]. The impedance spectra for cells made of electrodes with different carbons show that the formation of discharge products increases the impedance of the covered electrode. The relaxation loops related to the internal resistance of the cell increases with increase in the pore volume and surface area of the carbon showing larger surface area and larger pore volume provide more reaction sites for discharge reaction and more space for the accommodation of discharge products respectively. This increase in the cell resistance is due to the low conductivity of the discharge products [30]. These results show the qualitative improvement in lowering the impedance response of the lithium oxygen cell by tailoring the porous structure of the carbon used in the air cathode electrode.

The results of impedance measurements of ACRF600- 1123K carbon for discharge cycles following the first discharge cycle are shown in Figure 5. The semicircles related to the surface condition of the electrodes become larger with increasing cycle number showing an increase in interfacial impedance probably due to the irreversible deposition of some products at the interface of electrodes. The internal resistance of the cell increases with repeating charge and discharge cycles. This might hinder the passage of lithium ions to the electrode surface where oxygen is reduced catalytically, and subsequently impede the discharge reaction in the air electrode.

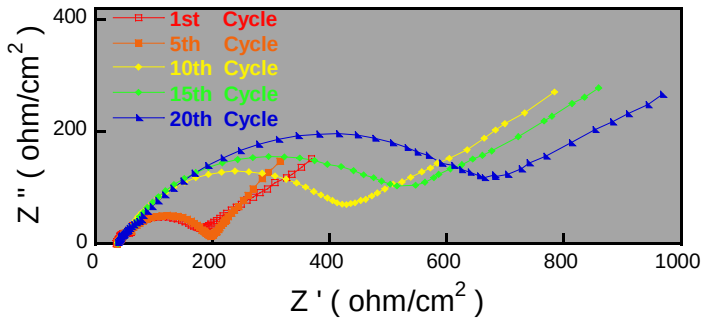

Fig 5. Impedance spectra of ACRF600-1123 carbon with cycling tests (rate 70 mA/g).

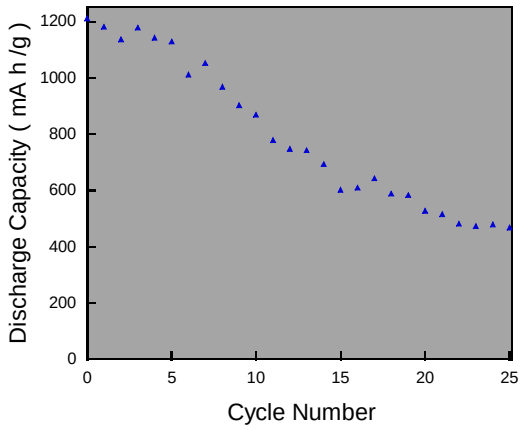

Fig 6. Variation of discharge capacity with cycle number for ACRF600-1123 carbon.

It is believed that as the cell discharges, Li_2O_2 deposited in the pores of the carbon changes the porosity of the electrode, and therefore the ability of oxygen and lithium ions to diffuse into the electrode.

Figure 6 shows change in the discharge capacity of the cell with cycle number for the first 25 discharge cycles. Increase in the cell impedance with cycle number shows that large surface resistances to electron or ion transfer will result in slow kinetics, large activation polarizations and lead to loss of cycling efficiency and capacity fading [31]. In fact the presence of resistive layers formed on the cathode surface may result in reduction of ion transfer at the electrode to levels where their concentration can no longer support the current demand. The lack of electron transfer must be compensated by removing some electrons from other species in the cell (i.e. electrolyte) leading to capacity fading and loss of cycling efficiency.

CONCLUSIONS

Air cathode electrodes based on RF carbon aerogels with controlled porous structure at nano scale, were prepared and their electrochemical performance in a lithium oxygen cell was evaluated by galvanostatic charge/discharge cycling and in situ impedance spectroscopy.

Galvanostatic charge/discharge measurements showed that the storage capacity of a lithium oxygen cell increases with the development of mesoporosity in carbon used in the cathode electrode suggesting that the structure of carbon is a key factor affecting the lithium oxygen cell performance.

EIS results demonstrate that the shape and value of the resistance in the impedance spectrum of Li/O_2 cell is strongly affected by the structure of the cathode. Gradual increase in the cell impedance with cycling, changes the porosity of the electrode and therefore the ability of oxygen and lithium ions to diffuse into the electrode, probably due to the irreversible deposition of some discharge products in the pores of the carbon. This will result in slow kinetics, large activation polarizations and lead to loss of cycling efficiency and capacity fading. So, it is important to minimize diffusion barriers and ionic and electronic resistances to decrease the internal resistance by tailoring carbon electrodes having appropriate porous structures and pore sizes that facilitate electrolyte and oxygen accessibility to the porous network.

ACKNOWLEDGMENTS

This work was funded by the EPSRC as part of the Supergen Energy Storage Consortium (Grant code EP/D031672/1).

REFERENCES

[1] W. Hermann, P. Bosshard, E. Hung, R. Hunt, and AJ Simon, *A technical assessment of high-energy batteries for light-duty electric vehicles*, Global Climate & Energy Project, Stanford University, USA, 2006.
[2] A. Debart, J. Bao, G. Armstrong, P.G. Bruce, *J. Power Source*s, 9 , pp. 1177-1182, 2007.
[3] M. S. Whittingham, *Chem. Rev.*, 104, pp. 4271-4301, 2004
[4] J.R. Akridge, Y.V. Mikhaylik, N. White, *Solid State Ionics*,175, pp. 243–245, 2004.
[5] Y. Talyosef, B. Markovsky, G. Salitra, D. Aurbach, H.-J. Kim, S. Choi, *J. Power Sources*, 146, 664–669, 2005.
[6] K. Kang, Y. S. Meng, J. Breger, C. P. Grey, G. Ceder, *Science*, pp. 311, 2006.
[7] M. Yoshio, S. Kugino, N. Dimov, *J. Power Sources*,153, pp. 375–379, 2006.
[8] J. Zhang and Y, Xia, *J. Electrochem. Soc.*, 153, pp. A1466-A1471, 2005.
[9] G. G. Amatucci, F. Badway, A. Singhal, B. Beaudoin, G. Skandan, T. Bowmer, I. Plitz, N. Pereira, T. Chapman, and R. Jaworskia, *J. Electrochem. Soc.*, 148, pp. A940-A950, 2001.
[10] A. Débart, L. Dupont , R. Patrice, J. M. Tarascon, *Solid State Sciences*, 8, pp. 640–651, 2006.
[11] J. Shim, K. A. Striebel, and E. J. Cairns, *J. Electrochem. Soc.*, 149, pp.A1321-A1325, 2002.
[12] X. Zhu, Z. Wen, Z. Gu, Z. Lin, *J. Power Sources*, 139, pp. 269–273, 2005.
[13] S. Zaromb, *J. Electrochem. Soc.*, 109, pp.1125-1129, 1962.
[14] D. Linden, B.T. Reddy, *Hand book of batteries*, 3rd ed., McGraw-Hill, New York, 1989.
[15] G. Q. Zhang, X. G. Zhang , Y.G. Wang, *Carbon*, 42, 3097–3102, 2004.
[16] W. Li, C. Li, C. Zhou, H. Ma, and J. Chen, *Angew. Chem.*, 118, pp. 6155 –6158, 2006.
[17] G. G. Kumar, N. Munichandraiah, *Electrochim. Acta*, 44, pp. 2663-2666, 1999.
[18] A. Patrick, M.Glasse, R. Latham and R. Linford, *Solid State Ionics*, 18 & 19, pp. 1063-1067, 1986.
[19] K. W. Semkow and A. F. Sammeils, *J. Electrochem. Soc.*, 134, pp. 2084-2085, 1987.
[20] J. J. Xu , H. Ye, *Electrochem. Commun.*, 7, pp. 829–835, 2005.
[21] E. L. Littauer and K. C. Tsai, *J. Electrochem. Soc.*, 124, pp. 850-855, 1977.
[22] K. M. Abraham and Z. Jiang, *J. Electrochem. Soc.*, 143, pp.1-5, 1996
[23] T. Ogasawara, A. Debart, M. Holzapfel, P. Novak, P.G. Bruce, *J. Am. Chem. Soc.*, 128 , pp. 1390-1393, 2006.
[24] J. Read, *J. Electrochem. Soc.*, 149, pp. A1190-A1195, 2002.
[25] M. Mirzaeian, and P. J. Hall, *Journal of Power System Technology*, 31, pp. 90-97, 2007.
[26] M. Mirzaeian, and P. J Hall, *Journal of Materials Science*, 44, pp. 2705-2713, 2009.
[27] S. J. Gregg, K. S. W Sing, *Adsorption, surface area and porosity*, Academic Press, New York, 1967.
[28] J.Y. Song, H.H. Lee, Y.Y. Wang, C.C. Wan, *J. Power Sources*, 111, pp. 255–267, 2002
[29] F. Croce, F. Nobili, A. Deptula,W. Lada, R. Tossici, A. D'Epifanio, B. Scrosati, R. Marassi, *Electrochem. Commun.*, 1, pp.605–608, 1999.
[30] X. Yang & Y. Xia, J Solid State Electrochem (2009) doi:10.1007/s10008-009-0791-8.
[31] G. Nazri, G, Pistoia, *lithium batteries*: *Science and Technology*, pp. 604-610, Springer, 2004